



ELSEVIER

Contents lists available at [ScienceDirect](https://www.sciencedirect.com)

# Case Studies in Construction Materials

journal homepage: [www.elsevier.com/locate/cscm](http://www.elsevier.com/locate/cscm)

## Case study

# Characterization of novel lightweight self-compacting cement composites with incorporated expanded glass, aerogel, zeolite and fly ash

Suman Kumar Adhikary<sup>a,\*</sup>, Žymantas Rudžionis<sup>a</sup>, Simona Tučkutė<sup>b</sup>

<sup>a</sup> Faculty of Civil Engineering and Architecture, Kaunas University of Technology, Kaunas LT - 44249, Lithuania

<sup>b</sup> Center for Hydrogen Energy Technologies, Lithuanian Energy Institute, Breslaujos st. 3, 44403 Kaunas, Lithuania

## ARTICLE INFO

### Keywords:

Aerogel  
Self-compacting cement composite  
Expanded glass  
Lightweight concrete  
Microscopy  
Porosity

## ABSTRACT

This study is aimed at preparing thermal insulating lightweight self-compacting cement composites (LWSCCC) below the density of  $1400 \text{ kg/m}^3$  by using lightweight minerals and aggregates. Study results showed that incorporation of porous-structured expanded glass aggregate (EGA) enhances the demand for water to maintain the workability and increases the risk of higher water absorption capacity. The use of a portion of aerogel as a replacement of EGA increases porosity by 7.3%, resulting in lowering of compressive strength by 49% and a 7% increase in water absorption capacity. However, the use of aerogel in combination with EGA cement composite can reach a density of less than  $1000 \text{ kg/m}^3$ , maintaining self-compaction ability and adequate strength. The gaps between the cementitious materials and aerogel shown in SEM indicate poor aerogel particle adhesion with cementitious materials. Additionally, X-ray diffraction analysis and thermal conductivity results were analyzed in this study.

## 1. Introduction

An intense rise in energy consumption and growing waste disposal problem has attracted researchers worldwide to consume waste materials for the sustainable growth of economy and the society. One of the interesting topic is thermal insulating composites that emerges from the use of waste materials, EGA is one such thermal insulating material usually prepared from waste/recycled glass [1]. These highly porous granules are primarily used to prepare lightweight composites bearing superior thermal and acoustic resistance, and much lighter density over conventional concrete [2]. During the last ten years, plenty of research has been carried out on normal weight SCC, while only a few studies have been conducted on the characterization of thermal insulating LWSCCC [3,4]. It is an optimized product of SCC and LWAC that facilitates the zero-required vibration energy for molding and casting. The development of LWSCC/LWSCCC not only provides great quality of product, but it significantly enhances the productivity and working environment. Therefore, the design of thermal insulating LWSCCC is imperative as an engineering and scientific incentive for future applications in energy-efficient buildings.

In past, some studies have been performed to evaluate the characteristics of lightweight aggregate concrete. Choi et al. [5] prepared high-strength LWSCC with a density range of  $2000\text{--}2300 \text{ kg/m}^3$ , and reported the correlation between strength and workability. The authors observed that increasing the concentration of fine LWA has a significant negative impact on obtaining adequate workability.

\* Corresponding author.

E-mail address: [sumankradk9s@gmail.com](mailto:sumankradk9s@gmail.com) (S.K. Adhikary).

<https://doi.org/10.1016/j.cscm.2022.e00879>

Received 16 October 2021; Received in revised form 5 January 2022; Accepted 8 January 2022

Available online 12 January 2022

2214-5095/© 2022 The Author(s). Published by Elsevier Ltd. This is an open access article under the CC BY license

(<http://creativecommons.org/licenses/by/4.0/>).

### Nomenclature

LWSCCC	lightweight self-compacting cement composites
LWA	lightweight aggregate
LWAC	lightweight aggregate concrete
EGA	expanded glass aggregates
OPC	Ordinary Portland cement
ITZ	Interfacial transition zone
EFNARC	European federation of national associations representing for concrete
SEM	Scanning electronic microscopy
XRD	X-ray diffraction analysis

Kwasny et al. [6] reported that in the case of semilightweight self-compacting concrete, larger grain LWA might float at the top and impact the homogeneous distribution of aggregates, resulting in segregation problems. Similar phenomena were observed by Adhikary and Rudzionis [7]. Yu et al. [8] prepared LWSCCC with a density range of 1280–1290 kg/m<sup>3</sup> using EGA and reported that the composite sample containing greater concentrations of EGA enhances the total permeable porosity. The authors also noticed that the selection of finer EGA has lower thermal conductivity and a more homogeneous aggregate distribution than coarse EGA. Interestingly, Adhikary et al. reported that fine EGA particles have higher strength properties relative to coarse particles. Lightweight concrete generally tends to have lower strength properties, depending on the lightweight aggregate used. Owing to low thermal and high strength properties, fine EGA particles become an interesting material to be used in lightweight concrete [7]. Aerogel is another thermal insulating material that has gained plentiful recognition for its applications in cementitious composites [9–11]. Gao et al. [12] prepared LWAC using aerogel and reported a weaker ITZ between the aerogel and cementitious composites, which might be attributed to the hydrophobic surface of aerogel. Adhikary et al. [13,14] reported that the presence of the gaps in the weaker ITZ of aerogel might enhance the porosity of the composites, leading to weaker strength and a risk of higher water absorption properties.

The literature studies suggest the detailed mechanical and durability properties of EGA and aerogel concrete. Aerogel and EGA both lightweight thermal insulating materials, and in the past, there were limited studies conducted evaluating the properties of EGA-aerogel cement composites. EGA has a thermal conductivity of about 0.052–0.077 W/(m-k) [1], whereas aerogel is much lighter and a thermal insulator than EGA, with a thermal conductivity of about 0.01–0.020 W/(m-k) [13]. The combination of aerogel and EGA significantly might lower the density of the cement composite and improves the thermal resistance performance. This kind of thermal insulating cement composite can be a useful product to use in different thermal bridges of buildings to improve the thermal insulation properties. It is very difficult to compact and transport the conventional thermal insulating cement composites in the conjoined part of buildings, while self-compacting thermal insulating cement composites might be a beneficial product to tackle these problems. Besides, aerogel is a highly fire and heat-resistant material, and the use of aerogel-based cement composites might provide protection from fire and heat [15–17]. Several studies in the literature indicate the presence of various materials-based thermal insulating lightweight cement composites; however, no studies have been conducted to evaluate the properties of EGA-aerogel-based thermal insulating self-compacting cement composites. So, this study is aimed at preparing lightweight thermal insulating self-compacting composites using EGA and aerogel below the density of 1400 kg/m<sup>3</sup>. Aerogel is much lighter than EGA, and the replacement of a partial amount of EGA with aerogel might significantly lower the density. To achieve the objective of the study, 1–2 mm and 0.5–1 mm of EGA were replaced with 0.5–2 mm of silica aerogel by 25%, 50%, 75%, and 100%. Aerogel is still a high-cost product on the market today, and using a higher concentration in cement composite could significantly increase production costs. This experimental study aims at the detailed analysis of self-compacting cement composites prepared using EGA and an adequate amount of aerogel with the use of supplementary cementitious materials.

**Table 1**  
Physical properties of expanded glass.

Designation	Standard	Expanded glass aggregate size			
		1–2 mm	0.5–1 mm	0.25–0.50 mm	0.1–0.3 mm
Particle density in Mg/m <sup>3</sup>	EN 1097-6:2003, C annex	0.37	0.42	0.52	0.57
Bulk density in kg/m <sup>3</sup>	EN 1097-3	230	270	340	400
WATER absorption % by mass (absorption % after 24 h submerged in water)	EN 1097-6:2002 C annex	18	18	15	10
Compression strength (±15%)	EN 13055–1, A annex	2	2.3	2.5	2.8
Thermal conductivity in W/(m-k) (±0.02)	EN 12939:2002	0.0663	0.0713	0.0767	0.0767
pH value		9–11			
Softening point		700 °C/1300°F (approximately)			
Color		Cream white			

**Table 2**  
Chemical properties of cement, zeolite, fly ash and EGA.

Chemical composition	CaO	MgO	SiO <sub>2</sub>	Al <sub>2</sub> O <sub>3</sub>	Fe <sub>2</sub> O <sub>3</sub>	K <sub>2</sub> O	Na <sub>2</sub> O	SO <sub>3</sub>	TiO <sub>2</sub>	Cl	Na <sub>2</sub> O eq	LOI	Insoluble residue	Free Lime	Lime paste	Other
Cement	63	2.9	20.4	4.1	3.5	0.7	0.23	3.2	—	0.03	0.74	2.5	0.5	1.2	3.9	—
Zeolite	2.8	0.7	58.7	9.0	1.4	2.6	—	0.1	0.2	—	—	5.1	—	—	—	—
Fly ash	3.68	1.7	49.7	27.45	7.38	4.54	0.95	0.92	1.65	—	—	—	—	—	—	2.03
EGA	8–10.5	—	71–73	1.5–2	<0.3	—	13–14	—	—	—	—	—	—	—	—	<0.5

**Table 3**  
Mixing composition of LWSCCC, kg/m<sup>3</sup>.

Mix	Cement	Sand	Aggregate (1/2 +1/0.5 +0.5/0.25 +0.01/0.3)	Aerogel	Zeolite	Fly ash	mva		Super plasticiser		Water	
							%	Kg/m <sup>3</sup>	%	Kg/m <sup>3</sup>	Kg/m <sup>3</sup>	w/b
A	550	380	45 + 56 + 44 + 56	–	–	–	1.8	0.327	1	5.5	247	0.45
B	530.2	183.16	43.4 + 54 + 42.4 + 43.6	–	–	–	1.73	0.327	1.30	6.9	308.5	0.58
C/Control	524.7	–	47.7 + 59.4 + 46.6 + 155.2	–	58.3	–	1.9	0.362	1.658	8.7	321	0.55
D	524.7	–	47.7 + 59.4 + 46.6 + 155.2	–	–	58.3	1.9	0.362	1.658	8.7	321	0.55
E	524.7	–	47.7 + 59.4 + 46.6 + 155.2	–	29.15	29.15	1.9	0.362	1.658	8.7	321	0.55
A25	524.7	–	35.8 + 44.5 + 46.6 + 155.2	8.01	58.3	–	1.9	0.362	1.658	8.7	321	0.55
A50	524.7	–	23.9 + 29.7 + 46.6 + 155.2	16.02	58.3	–	1.9	0.362	1.658	8.7	321	0.55
A75	524.7	–	11.9 + 14.9 + 46.6 + 155.2	24.03	58.3	–	1.9	0.362	1.658	8.7	321	0.55
A100	524.7	–	0 + 0 + 46.6 + 155.2	32.04	58.3	–	1.9	0.362	1.658	8.7	321	0.55

## 2. Materials and methods

### 2.1. Materials

OPC (CEM I 42.4R), fly ash, and zeolite powder (50  $\mu\text{m}$ ) were used as mineral admixtures, and expanded glass and aerogel were used as LWA to produce LWSCCC. The physical properties of EGA and the chemical composition of fly ash, zeolite, cement, and EGA are presented in [Tables 1](#) and [2](#), respectively. In the LWSCCC, MasterMatrix SDC 100 stabilizer and polycarboxylate based superplasticizer MasterGlenium SKY 8700 were used as chemical admixtures.

### 2.2. Sample preparation

The composite samples were prepared using mixing and trial methods. Composite mixture A was prepared using combinations of natural sand and 0.1–0.3 mm, 0.25–0.50 mm, 0.5–1 mm, and 1–2 mm size EGA. To prepare the composite specimen A, SCLC1 sample composition was taken as a reference sample from the experimental study by Yu et al. [8]. To lower the density of the composite, natural sand was replaced with 0.1–0.3 mm EGA. Due to the increase in fine content, the demand for water increased to maintain the desired workability. For the composite samples C, D, and E, a small amount of SCM such as zeolite and fly was used to improve the workability of the composite.

From the visual inspection of workability and analysis of strength, density, and water absorption results, zeolite was chosen as the SCM to prepare the next aerogel-added composite specimens. Composite sample C was considered as the control sample, and 0.5–1 and 1–2-mm EGA aggregates were replaced with 0.5–2 mm of aerogel particles (70  $\text{kg}/\text{m}^3$  bulk density) by volumes of 25%, 50%, 75%, and 100%. The water/binder ratio of all composite samples was maintained at 0.55. The mixing composition of all LWSCCC is presented in [Table 3](#). During the mixing process, first EGA, zeolite powder, and cement were carefully mixed in the dry state. Then 70% of the total water content was added to the mixture and manually mixed for 3 min. Thereafter, the superplasticizer and stabilizer are mixed with the remaining water and added to the composite mixture. At the last stage, aerogel was added to the composite mixture to minimize the crushing of aerogel particles, then mixed for another 2 min.

### 2.3. Workability test

The fresh properties of lightweight self-compacting cement composite, such as mini-slump flow, slump flow, mini v-funnel, and V-funnel time, were immediately measured according to the EFNARC guidelines [18]. A slump cone with a 30 cm height, a 20 cm bottom diameter and a 10 cm top diameter used to test slump flow. While performing mini-slump flow on a flow table with a 6 cm height, a 10 cm bottom diameter, and a 7 cm top diameter was used. In the slump-flow and mini-slump flow tests, the slump cone and flow table cone were lifted vertically. After the flow stopped, the mean diameter of the composite base was taken as a result. V-funnel test of the composite was performed using a V-shaped funnel satisfying dimensions of the EFNARC guidelines for concrete and mortar. After filling the fresh composite bottom opening of the V-funnel was opened after 10 s and flow out time was measured. Subsequently, samples were molded into 16.0  $\times$  4.0  $\times$  4.0 cm size prisms for the hardening process and kept in the open air for 24 h. Hardened composite specimens were demolded and kept in water for the hydration process in the climatic chamber (RH: more than 95%, room temperature 20  $\pm$  1  $^\circ\text{C}$ ) for 28 days.

### 2.4. Compression and flexural strength

Compression and flexural strength of LWSCCC were tested on the 28th day of hydration satisfying the EN 196-1:2016 standard. On the 28th day, water immersed composite specimens were taken out from the climatic chamber and kept at room temperature for 6 h for the natural drying process and afterwards, used in the mechanical strength test. A total of 6 specimens for each sample were tested, and the average value was considered as a result.

### 2.5. Density and water absorption

After the hydration process on the 28th day, the composite specimens were taken out of the water and kept in the oven at 105  $^\circ\text{C}$  for 24 h. After 24 h of the oven drying process, the dry density of each type of composite specimen was measured. Afterward, the composite specimens were immersed in water for 15 min, 1 h, 24 h, and 48 h to measure the water absorption capacity of the composite specimens. The average value of six specimens of each type of composite sample was taken as the final result.

### 2.6. Porosity

The porosity of LWSCCC samples was calculated after 28 days of hydration according to the GOST 127304 standard. To determine the porosity of the composite, first the composite samples were oven dried at 105  $^\circ\text{C}$  for 24 h. The mass of the oven-dried samples was measured using highly accurate equipment. Afterwards, composite samples were kept in water, immersed for 15 min, 1 h, 24 h, and 48 h; the subsequent mass of the water-immersed samples was measured after 15 min, 1 h, 24 h, and 48 h, respectively. Finally, after 48 h of water absorption, the masses of the samples were measured under the water, and using a flowing formula, the total and open porosity of the composite were calculated.

Ordinary density ( $\text{kg/m}^3$ ) =  $\{\text{Mass of oven dried sample}/(\text{mass of the water immersed sample after 48 h water absorption} - \text{mass of the sample under water})\} * 1000 \dots (1)$ .

Massive water absorption (%),  $W_p = (\text{mass of the water immersed sample after 48 h of water absorption} - \text{mass of the oven dried sample}) / \text{mass of the oven dried sample} * 100 \dots (2)$ .

Open porosity (%) =  $(\text{massive water absorption} * \text{ordinary density}) / 1000 \dots (3)$ .

Total porosity =  $\{1 - (\text{ordinary density} / 2690)\} * 100 \dots (4)$ .

Closed porosity =  $\text{total porosity} - \text{open porosity} \dots (5)$ .

## 2.7. Thermal conductivity

The thermal conductivity of LWSCCC specimens was calculated by EN 1745:2012 standards. On a side note, this calculation is based on the density of lightweight aggregate concrete. The aggregate-matrix transition zone, type of aggregates, and presence of fly ash and zeolite might have notable impacts on the thermal conductivity of the composite. Aerogel is a highly thermal insulating material, having greater thermal resistance than EGA. The actual thermal conductivity of the aerogel-added lightweight cement composite tested in the laboratory is expected to have a lower thermal conductivity than the obtained results from the calculation.

## 2.8. Scanning microscopy

SEM of LWSCCC specimens was analyzed by a high-resolution electronic microscope Hitachi S-3400 N with a Bruker Quad 5040 EDS detector (123 eV). A thin layer of concrete slice was cut from the cement composite using a rotary blade cutter at the age of 28 days for the microscopic analysis.

## 2.9. X-RD

The DRON-6 X-ray diffractometer was used to perform the X-ray diffraction analysis of cement, fly ash, zeolite, and LWSCCC composite specimens. The operating voltage of the equipment was 30 Kv with 20 mA current emission, and each step scan of  $2\theta$  was  $0.02^\circ$ . Fracture pieces of the cement composite generated from the compressive strength test were selected for the XRD analysis at the age of 28 curing days. Fragmented pieces of the cement composites were powdered manually using ceramic-made apparatus, and the samples were sent for the XRD test.

## 3. Results

### 3.1. Workability

The workability results of LWSCCC are presented in Table 4. Study results indicate that composite mixture D, prepared with fly ash, shows the highest flow diameter. While LWSCCC mixture A shows the lowest workability compared to other specimens. Mini-slump flow and mini-V-funnel time of samples A, B, C, D, and E lay between 247 and 258 mm and 7.2 to 9 s. The increase in fine EGA content in composite mixture B increases the demand for water and superplasticizer doses to maintain the workability of LWSCC. Also, EGA has a higher water absorption capacity than natural aggregates, which might lead to an increase in demand for water/superplasticizer doses [1,19–21]. However, composite samples C, D, and E showed improved workability, and this might be due to the addition of fine pozzolans and increased superplasticizer doses. Guneyisi et al. [22] and Ting et al. [23] reported the enhanced workability effects of fly ash added LWSCC. The addition of fly ash might have a dilution effect that diminishes the flocculation of the cement particles. Besides, spherical-shaped FA particles provide ball-bearing effects by facilitating the movement of neighboring particles. Perhaps due to a similar mechanism, enhanced workability was observed in this study.

The inclusion of aerogel and its concentration slightly negatively impacted the fresh properties of LWSCCC. With the rising concentration of aerogel replacement, the slump flow diameter is slightly reduced and the V-funnel time increases. At 100% replacement volume of aerogel by of 2/1- and 1/0.5-mm size EGA, the mini-slump flow diameter is almost lowered by 4.3%. A similar reduction in

**Table 4**  
Workability of LWSCCC.

Composite Mix	Flow table diameter, mm	V-funnel time, seconds (according to EFNARC guideline V-funnel dimensions for mortar)	Slump cone diameter, mm	V-funnel time, seconds (EFNARC guideline V-funnel dimensions for concrete)
A	247	9	720	6
B	248	8	725	5
C/Control	256	7.2	800	4
D	258	8	820	5
E	257	8.1	807	5
A25	256	8	795	5
A50	251	8.5	750	5.5
A75	247	9.2	717	6.1
A100	245	9.5	700	6.3

flowability of the aerogel added composite was observed in a previous studies [24,25]. Kim et al. [26] used aerogel powder in a thermal insulating mortar and reported a 37.8% reduction in flow. The surface chemicals of aerogel, carboxylic ( $-\text{COOH}$ ), and hydroxyl ( $-\text{OH}$ ), can also absorb some water, leading to a decrease in workability [13,27]. Perhaps due to a similar reason, a slight decline in workability of LWSCCC was noticed in this study. According to the EFNARC recommendations, mortars should have a flow diameter (flow table method) of 240–260 mm with a V-funnel time of 7–11 s. To satisfy the SCC criteria, concrete must have a 550–850 mm slump flow diameter and an 8–25 s V-funnel time. In the present study, all the prepared composite samples fulfilled the self-compactability criteria.

### 3.2. Porosity

The porosity of LWSCCC is an important factor that might have notable impacts on the strength and durability properties of the composite. Fig. 1 shows the general and open porosity of all LWSCCC specimens. The general (total) porosity and open porosity of the composites A to E lie between 50% and 56.93%; and 16% and 17%, respectively. The increase in water/binder ratio and EGA concentration increases the porosity of B, C, D, and E. EGA is a porous structured material, and incorporation of EGA at a high volume might enhance the total porosity of concrete [1,28,29]. Adhikary et al. [1] reported that after the evaporation of free water in cement composites, pores were created that enhanced the porosity of concrete. Due to the use of EGA and a higher water/binder ratio, the porosity of LWSCCC increased and led to lower strength properties. However, the addition of pozzolan materials didn't have a significant impact on the porosity of LWSCC.

The general and open porosity of all the aerogel added LWSCCCs was increased by the increases in the aerogel concentration. The general porosity of the control samples, A25, A50, A75, and A100, was measured at 56.93%, 58.77%, 60.22%, 62.08%, and 64.23%, respectively. The open porosity of the control samples, A25, A50, A75, and A100 was measured at 15.72%, 17.38%, 18.9%, 19.1%, and 19.32%, respectively. Figs. 1 and 2 show a clear relationship between the aerogel concentration, porosity, and strength. With the increase in aerogel content in the LWSCCC, the porosity increases, and the strength decreases. The enhancement in porosity of aerogel added LWSCCC can be explained as during the mixing process, hydrophobic aerogel entrapped some air bubbles, leading to a rise in porosity and a decline in strength [13]. It was [12,13] reported that due to its hydrophobic characteristic, aerogel has lower adhesion with cement paste, leading to microscopic separation gaps in the ITZ between aerogel and cementitious materials. Because of these phenomena, the porosity of the aerogel-based thermal insulating LWSCCC of this study can be enhanced. Lu et al. [30] reported that the use of 66 vol% of aerogel in cement composite could reach a porosity of around 72.8%. A similar increase in the porosity of aerogel added concrete was noticed by several authors [9,30,31]. EGA is a porous structured material and the use of it significantly increases the porosity of concrete [1,32,33]. Agreeing with previous literature, combinations of aerogel and EGA might lead to achieving such high porosity.

### 3.3. Density

Fig. 3 shows the density of all LWSCCC samples. The dry density of the composites A to E lies between 1343 and 1126  $\text{kg}/\text{m}^3$ . Study results show that the decrease in natural sand concentrations and the rise in EGA in the composite significantly decreased the density. EGA is a much more lightweight material than natural aggregate, and incorporation of a high concentration of EGA in a cement composite might lead to a decrease in density [8,34,35].

Study results also show the significant decrease in density of LWSCCC by the rise in aerogel concentration. The addition of aerogel as a 100% replacement of 1/0.5 and 2/1 mm EGA reduced the density of LWSCCC by 15.8%. The oven-dry density of the control samples, A25, A50, A75, and A100, was measured 1126, 1076, 1044, 1019, and 948  $\text{kg}/\text{m}^3$ . From the Fig. 4, it can be clearly understood that the concentration of aerogel, density, strength, and porosity share a close relationship. As the concentration of aerogel increases, the porosity also increases, leading to a decrease in the density and strength of LWSCCC. Zhu et al. [36] prepared lightweight concrete and measured a density of 1740  $\text{kg}/\text{m}^3$  without aerogel content that decreased to 582  $\text{kg}/\text{m}^3$  containing 80 vol% of aerogels. Similarly,

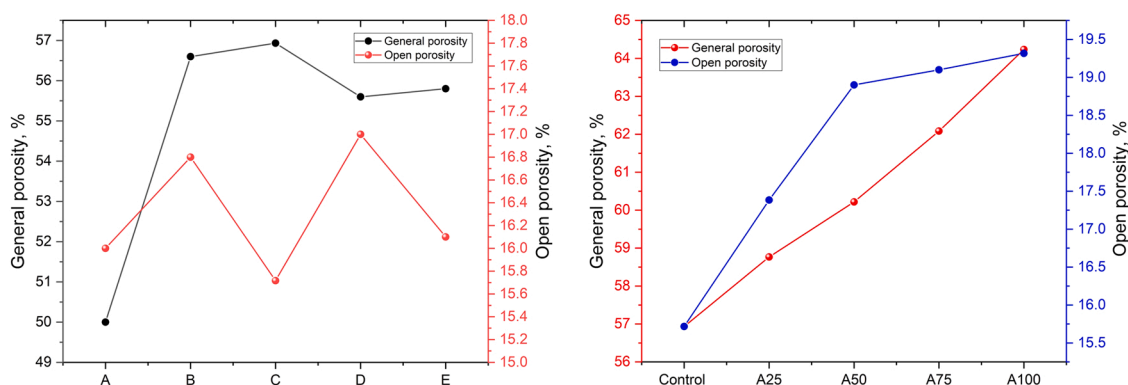


Fig. 1. General and open porosity of LWSCCC.

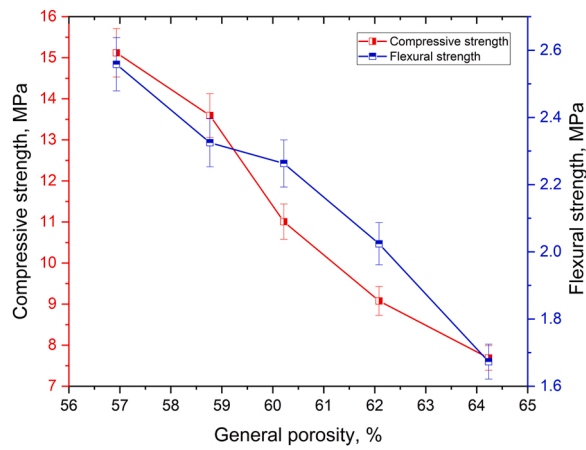


Fig. 2. Relationship between the general porosity and mechanical strength of aerogel added LWSCC.

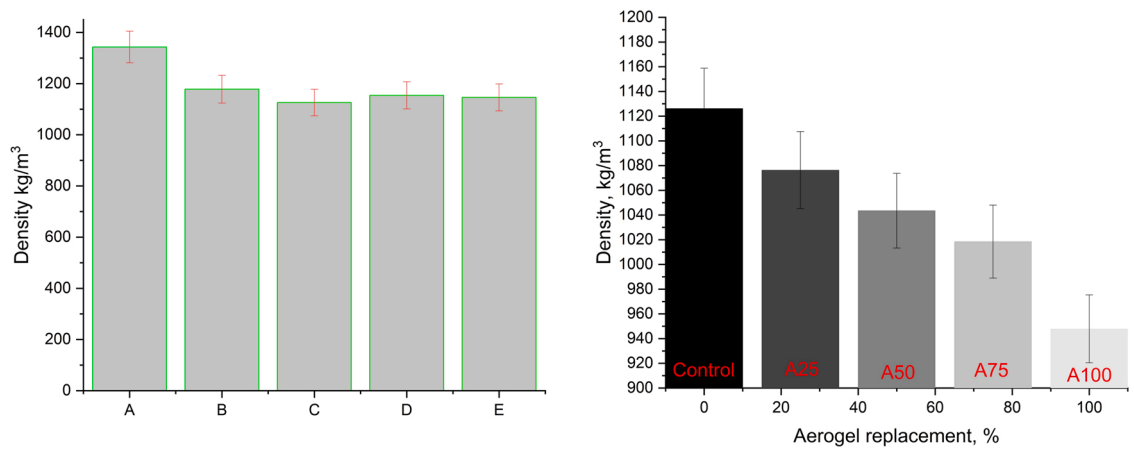


Fig. 3. Oven dry density of all LWSCC.

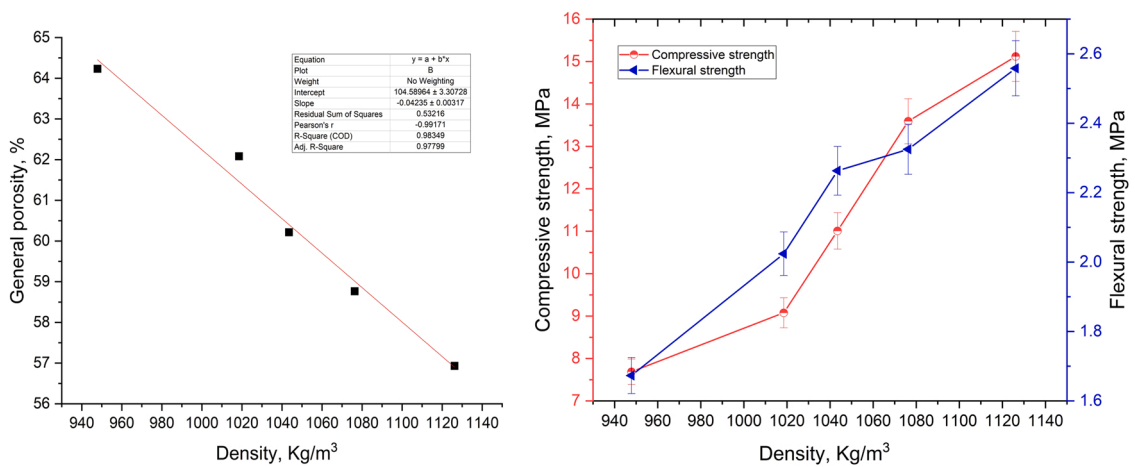


Fig. 4. Relationship between the porosity and density; and density vs mechanical strength of aerogel added LWSCC.



Liu et al. [37] reported that the use of 60 vol% of aerogel in mortar could decrease the density by about 38.9%. A similar decrease in density of aerogel added concrete was reported by several researchers [12,38–40]. EGA is also a very lightweight aggregate, and the use of EGA as LWA can significantly decrease the density of concrete [1,35,41].

### 3.4. Compression and flexural strength

The compression and flexural strengths of all LWSCCC samples are presented in Fig. 5. The compression and flexural strength of the composites A to E lie between 21.3 and 12.4 MPa; and 5.5 and 2.56 MPa, respectively. The LWSCCC sample A, prepared with the combination of sand and EGA, achieves the highest compressive and flexural strength. Increasing the EGA concentration in the composite decreases the mechanical strength. This phenomenon can be explained as a combination of sand and EGA showing better compatibility, leading to higher strength development. Besides porous structured EGA has lower mechanical strength, and a high volume of EGA in the concrete leads to a decrease in strength. [1,42–44]. Composite sample D prepared with fly ash shows slightly lower strength. This might be due to the retardation in the hydration of cement, leading to lower strength development at an early age [45]. However, zeolite-added composites show greater strength characteristics than fly ash-added composite D. Ahmadi and Shekarchi [46] reported that the use of 20% zeolite powder as a replacement for cement might enhance the compressive strength by 25%. A similar enhanced strength of zeolite added concrete was reported by Chan and Ji [47]. A comparatively higher water/binder ratio was used in the composite specimens B to E, and that could also be a reason for the decrease in strength. A similar decrease in the strength of foamed glass concrete by enhancing the water/binder ratio was observed by Limbachiya et al. [43] and Zach et al. [28].

The results of LWSCCC also indicate that with the rise in aerogel concentration, both compression and flexural strength were decreased. The decrease in compression strength was more significant compared to flexural strength. Adding 100% aerogel as a replacement of 1/0.5 and 2/1 mm EGA shows almost a 49.2% and 34.6% decrease in compression and flexural strength, respectively. The compression strength of the control samples, A25, A50, A75, and A100 was measured 15.12, 13.59, 11.01, 9.08, and 7.69 MPa respectively. The flexural strength of A25, A50, A75, and A100 was measured at 2.56, 2.33, 2.26, 2.02, and 1.67, respectively. The decline in the strength of aerogel added LWSCCC can be attributed to the brittleness of aerogel. Because of its fragile nature, aerogel cannot withstand sufficient loads [12,13,48]. A similar decrease in the strength of aerogel added concrete was reported by several researchers [12,24,38,49,50]. Besides, SEM images suggest that aerogel has lower adhesion with cement composites and that aerogel might entrap some airbubbles. Those phenomena might lead to an increase in porosity and a decline in strength. However, in a previous study [51], it was observed that the use of 0.6% nanotube in aerogel concrete could enhance the strength by 41.48%.

### 3.5. Water absorption

Water absorption of concrete is an important durability factor. Higher water absorption of concrete can allow unwanted substances into concrete that might hamper the durability characteristic of concrete. Lightweight aggregate concrete is mainly a porous material having with a higher porosity than conventional normal weight concrete. Fig. 6 suggests that the water absorption capacity of the composites A to E shows about 11.9–14.39% after a 48-hour absorption test. Composite specimens prepared with greater EGA concentrations shows higher water absorption. EGA is a porous-structured LWA that can absorb 20–25% of water, and the use of a high volume of EGA in concrete might enhance the water absorption [1]. Besides, the higher w/b of the cement composites might also lead to enhanced water absorption. After the evaporation, free water makes pores in the composite, leading to an enhancement in porosity and water absorption [1]. However, there was no significant impact of pozzolanic materials observed in this study.

Fig. 6 also revealed that the water absorption of the composites increases as the aerogel content increases. The final water absorption after 48 h of the control samples, A25, A50, A75, and A100, was measured at 13.57%, 15.67%, 17.70%, 18.74%, and 20.06%, respectively. This enhanced water absorption of aerogel-added cement composites might be attributed to the entrapped air bubbles by aerogel. Besides, aerogel has weaker adhesion with cementitious materials, and those entrapped air bubbles and separation gaps in ITZ might enhance the porosity of the composites, leading to an increase in water absorption [9,13,30,52,53]. The relationships of porosity

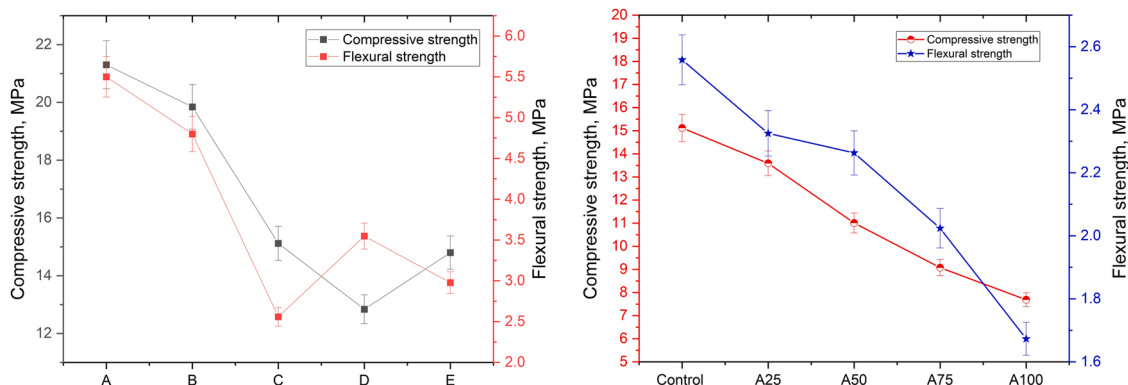


Fig. 5. Compression and flexural strength of LWSCCC.

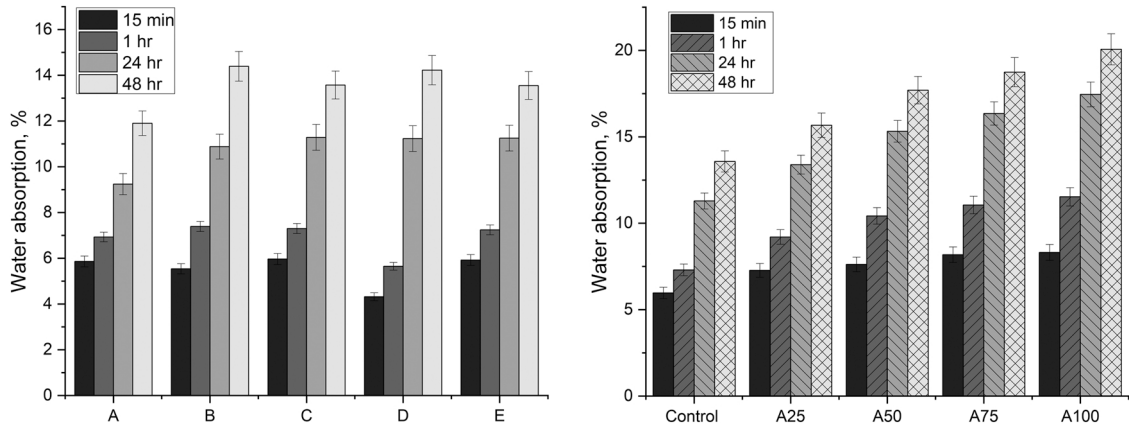


Fig. 6. Water absorption of all LWSCCC.

and water absorption of the aerogel cement composite presented in Fig. 7 satisfy those statements. Soares et al. [53] used aerogel in their study and reported an almost 56% increase in the open porosity of aerogel added cement mortar, leading to an enhancement in capillary water absorption. However, previous study results [51] suggested that the use of carbon nanotubes effectively enhances the adhesion between aerogel and cement paste in the ITZ, leading to improvement in the water absorption capacity of concrete.

3.6. Scanning microscopy

Aerogel is a brittle material, and Fig. 8 shows clearly visible cracks on the aerogel surface. Due to its hydrophobic nature, aerogel doesn't have good adhesion with cement paste resulting in a separation gap in the ITZ of aerogel and cementitious materials. The microscope image doesn't show any cracks or separation gaps in the ITZ between EGA and cement paste. The ITZ of aerogel and EGA are presented in Fig. 9. SEM images suggest that EGA has greater adhesion with cementitious materials compared to aerogel. Some pores were observed surrounding the aerogel particles in the LWSCCC as presented in Fig. 10. This can be attributed to the entrapped air bubbles by the aerogel during the mixing of fresh concrete [13]. The presence of pores and gaps in the ITZ of aerogel might increase the porosity of the composite and lower the strength. Besides, it allows harmful substances into the cement composites and impacts the durability characteristics. Some studies have reported that the use of silica fume and carbon nanotubes might improve the microstructure and ITZ of aerogel concrete [51,59]. A study [54] reported that a rim of air bubbles in the transition zone between EGA and the cement paste might have occurred during the exchange of air and water during the water absorption. However, in this study, it is evident that no rim of air bubbles were created in the ITZ of EGA. Fig. 9 also shows the presence of crystals of ettringites in the pores of EGA and in the ITZ. A similar observation was noticed by Bumanis et al. [55]. The authors also reported that during the mixing process, the outer shell of EGA might easily collapse due to its lower strength characteristics, leading to acceleration of the ASR mechanism. The presence of ettringite might promote the recrystallization of ettringite or leach out alkalis leading to deterioration and expansion of composite. Needle-shaped hydration products (ettringite) were observed in the aerogel added LWSCCC as shown in Fig. 11. However,

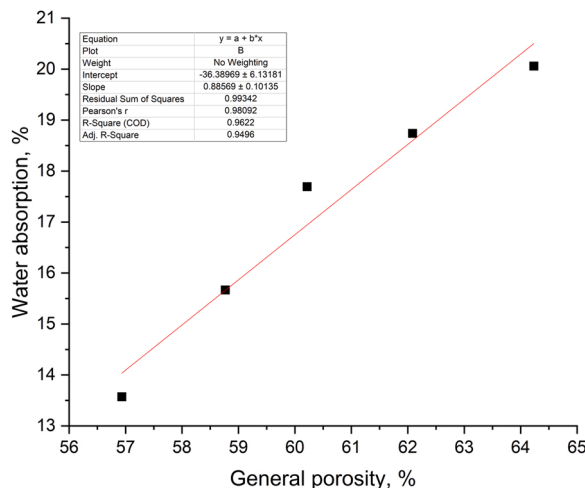


Fig. 7. Relationship between water absorption and general porosity of aerogel added LWSCCC.

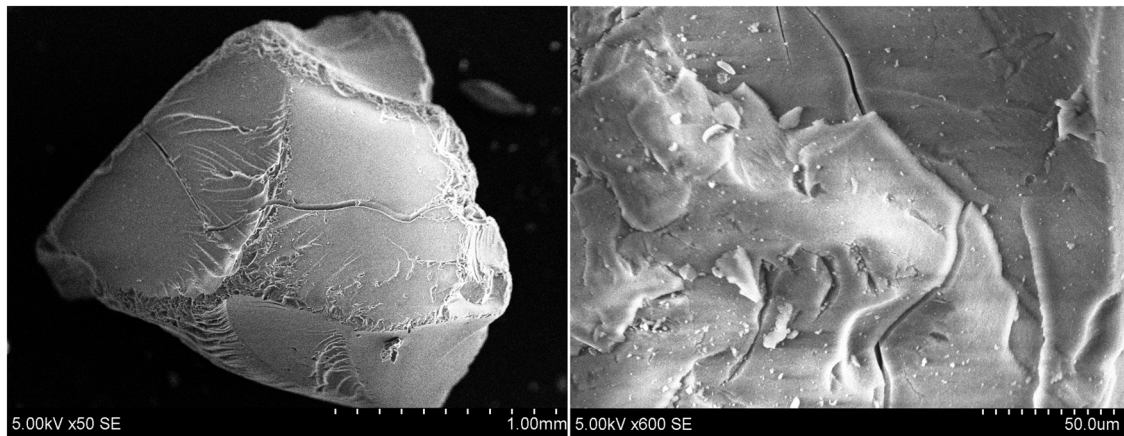


Fig. 8. Microscopic image of silica aerogel showing its cracked surface.

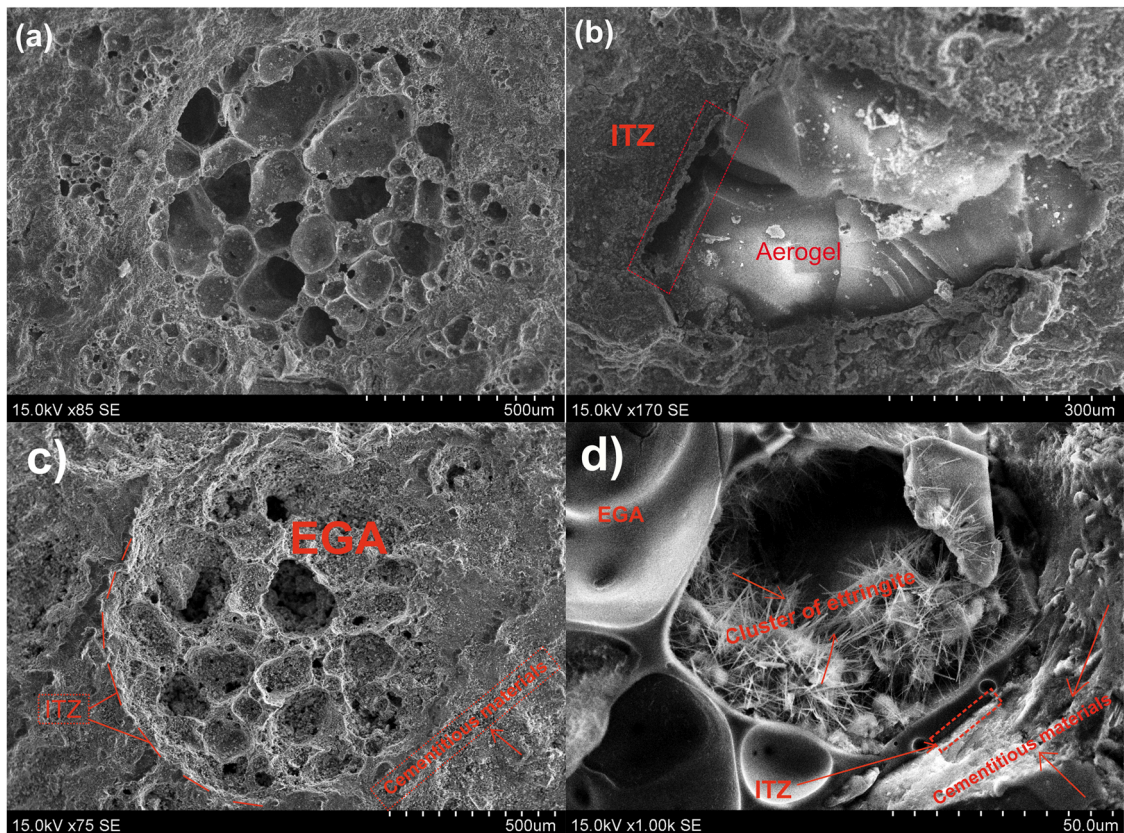


Fig. 9. Microscopic image of EGA and aerogel added cement composite showing the ITZ between the aggregate and cementitious composites.

the smooth and clean surface of the aerogel in composite specimen also indicates no degradation of aerogel due to the hydration of cementitious materials as presented in Fig. 9 (b) and Fig. 10 (d). This occurrence indicates that the aerogel particles might stay fairly stable during the hydration process of cement. Gao et al. [12] also observed a similar occurrence in their study. However, Zhu et al. [56] reported that aerogel particles might slightly dissolve in the alkaline environment provided by cement hydration and form C-S-H with a low Ca/Si ratio. Hai-li et al. [57] and De Fátima Júlio et al. [58] reported that the presence of amorphous silica in silica aerogel might lead to ASR due to the reactions between alkali presence in cement and the hydroxyl ions of aerogel.

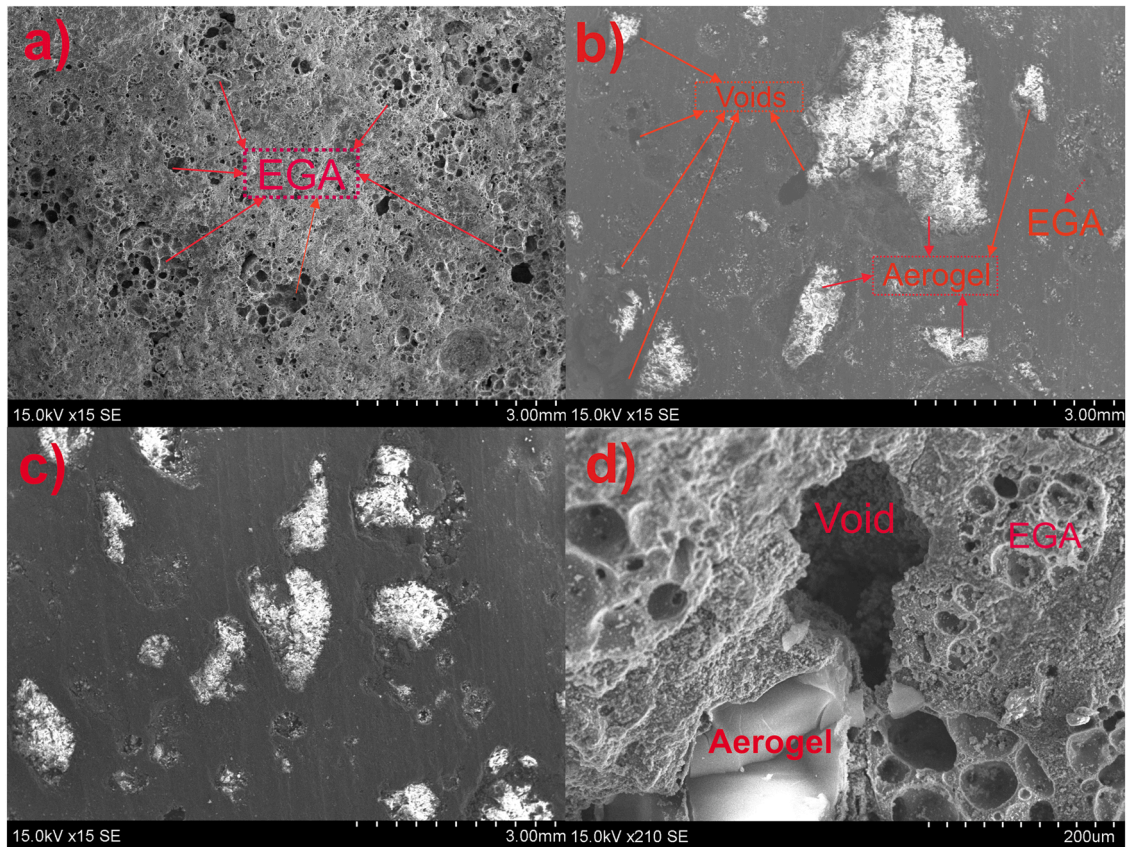


Fig. 10. Microscopic image of EGA and aerogel added cement composite showing the distribution of LWA and the entrapped voids surrounding to the aerogel particles.

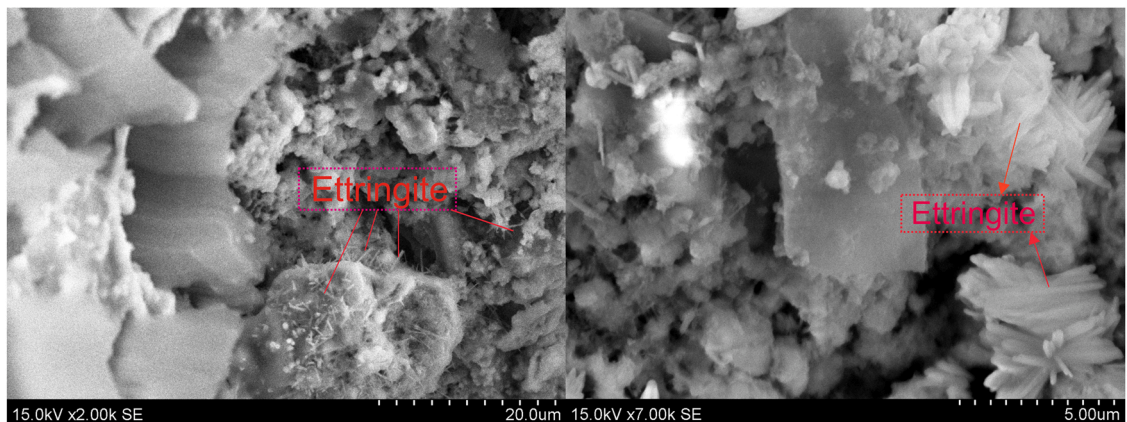


Fig. 11. Microscopic image of aerogel added cement composite (28 days) showing the growth of hydration products.

### 3.7. XRD analysis

X-ray diffraction patterns of OPC, fly ash, zeolite, and EGA are presented in Figs. 12, 13, 14, and 15. An XRD of EGA and aerogel confirms its amorphous characteristics, near  $23^\circ$  a hump was noticed. The XRD of LWSCCC samples A to E; and samples containing aerogel is presented in Figs. 16 and 17. The XRD of LWSCCC revealed that ettringite, portlandite, calcite, calcium aluminum silicate hydrate, calcite, brownmillerite, and lawsonite are the main hydration products of LWSCCC. It was observed that the intensity of ettringite near  $8^\circ$  for LWSCCC mix B was reduced compared to mix A. This reduction in ettringite content can be attributed to a higher

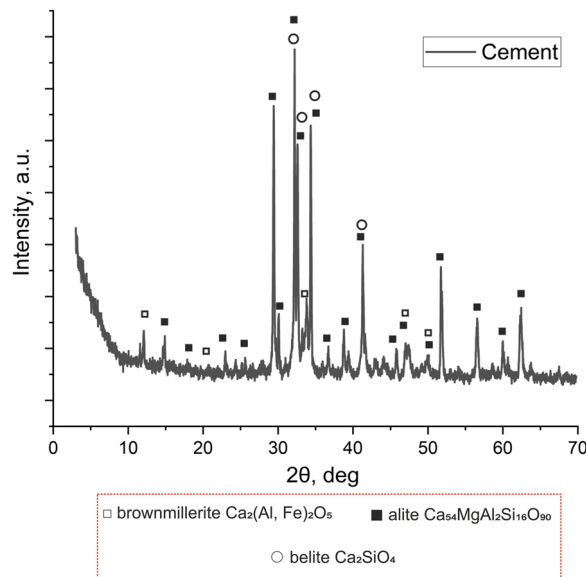


Fig. 12. XRD pattern of OPC cement.

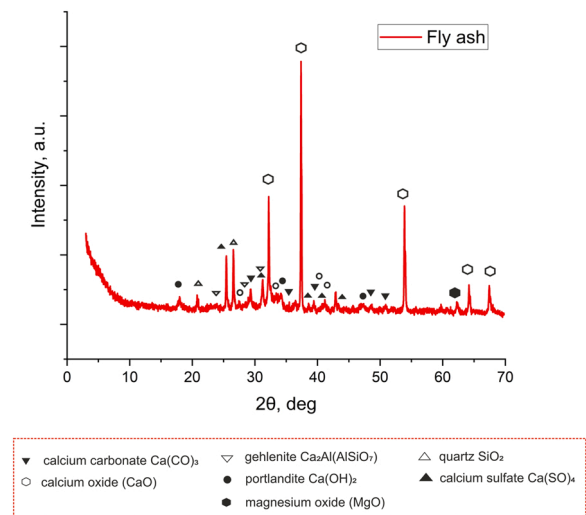


Fig. 13. XRD pattern of fly ash.

water/binder ratio.

Zuo et al. [60] reported a similar higher ettringite content at a lower water/cement ratio. The author also reported that higher growth of ettringite might help to enhance the compression strength of the composite. The reduced intensity of the LWSCCC mix can be attributed due to the delay in hydration provided by higher doses of PCES [61]. The peaks of portlandite near 18° and 34° were observed for all LWSCCC samples, while compared to fly ash added LWSCCC, a higher intensity of portlandite was observed for LWSCCC containing zeolite. The combination of fly ash and zeolite shows slightly higher peaks than the fly ash added composite samples. This can be attributed to the acceleration in pozzolanic reactivity due to the presence of zeolite. However, the enhanced peak of ettringite shows that the addition of zeolite might accelerate the formation of ettringite. A similar appearance of ettringite in zeolite added cement was observed by Snellings et al. [62]. The XRD image also shows higher peaks of ettringite and calcium aluminum silicate hydrate till 75% replacement volume of aerogel. A reduction peak was noticed for A100, containing a higher volume of aerogel. These phenomena suggest that aerogel might partially dissolve and react with OPC. Similar phenomena were observed by Zhu et al. [56].

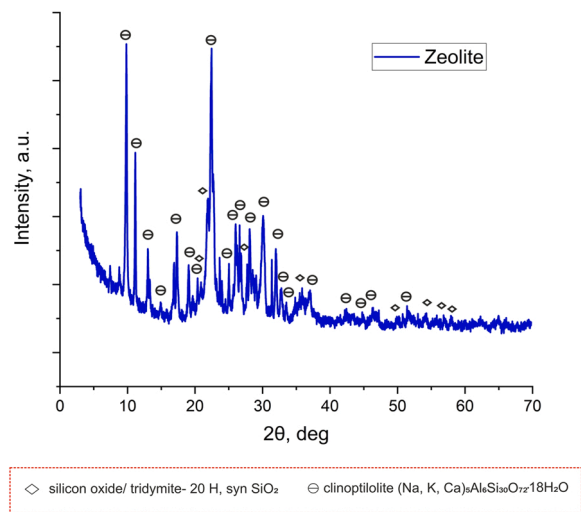


Fig. 14. XRD pattern of zeolite.

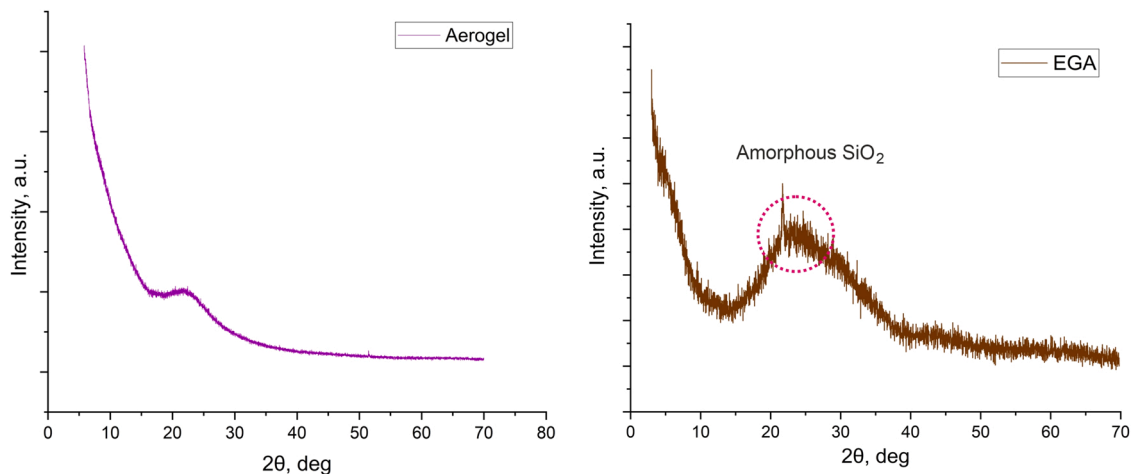


Fig. 15. XRD pattern of EGA and silica aerogel.

### 3.8. Thermal conductivity

The thermal conductivity coefficient of concrete is mainly density-dependent [8]. The thermal conductivity of normal weight concrete is about 1.6 W/m·K at 2200 kg/m<sup>3</sup> density. The thermal conductivity of all LSWCCC is shown in Fig. 18A higher concentration of EGA combined with zeolite lowers the density and enhances the total porosity of composite, leading to an improvement in thermal conductivity. It was also observed that an increase in aerogel content in the LWSCCC thermal conductivity of the composite specimen decreases. The thermal conductivity coefficient of the control samples, A25, A50, A75, and A100, was calculated as 0.47, 0.45, 0.427, 0.418, and 0.382 W/m·K, respectively. The addition of EGA and aerogel to LWSCCC significantly lowers the density due to a rise in porosity and their lightweight density [13,63,64].

Abbas et al. reported that the use of aerogel in lightweight thermal insulating composites could lower the thermal conductivity by 46% by adding 62.34 vol% of aerogel to the composite [9]. Similarly, Gao et al. [12] reported that with the addition of 60 vol% aerogel to the cement composite, 50% of the density of the composite was reduced and the thermal conductivity was reduced by around 7 times. A similar decrease in thermal conductivity of aerogel added cement composite/concrete was observed by several authors [9,49,50,64–66]. Fig. 18 and Fig. 19 show that aerogel content, porosity, density, mechanical strength, and thermal conductivity share a close relationship, as the aerogel content rises in the composite, porosity increases, whereas density, compressive strength, and thermal conductivity decrease.

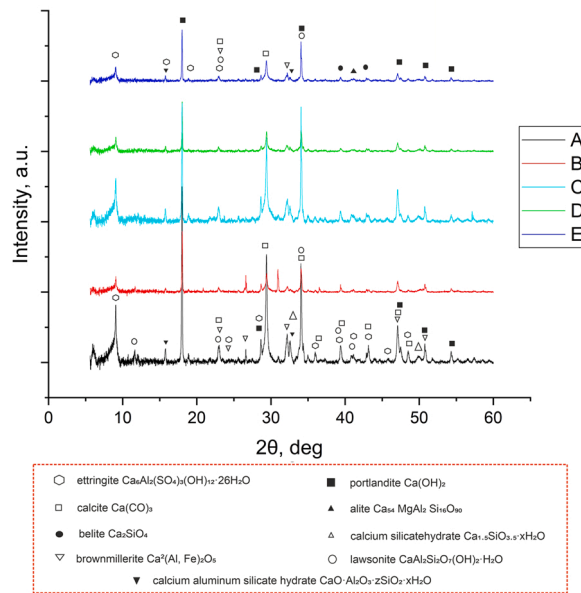


Fig. 16. XRD pattern of LWSCC composite specimen A to E.

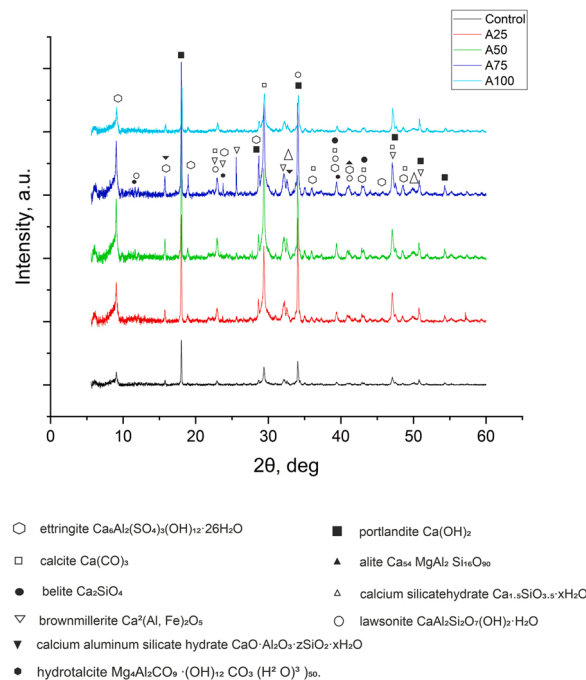
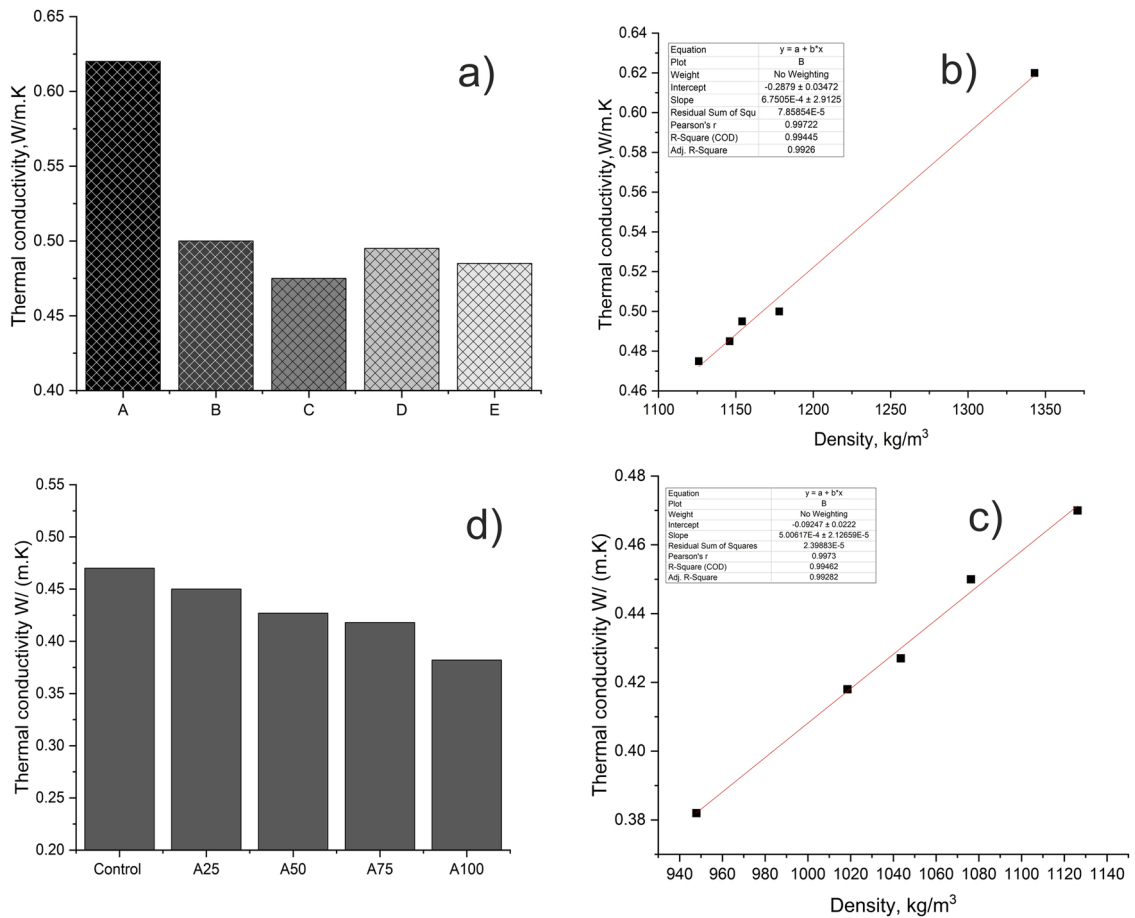


Fig. 17. XRD pattern of LWSCC composite specimens containing aerogel.

### 3.9. Discussion

EGA is a porous structured lightweight aggregate containing a high volume of pores within its structure. Because of the porous structure, EGA has very low strength and density compared to conventional natural aggregates. EGA's mechanical and physical properties might vary according to size, degree of porosity, and manufacturing process [51]. Due to the lightweight density, LWA might float to the top of the concrete mixture, impacting the homogeneous distribution of aggregates and leading to segregation [15, 16]. A study result reported that the use of fine particles and greater binding materials could improve the flowability of concrete [67]. Also, it was observed in a previous study that the use of combinations of fine EGA shows a greater homogeneous distribution of



**Fig. 18.** a) thermal conductivity of LWSCCC samples A to E; b) relationship between density and thermal conductivity of LWSCCC samples A to E. c) thermal conductivity of LWSCCC samples containing aerogel; d) relationship between density and thermal conductivity of LWSCCC samples containing aerogel.

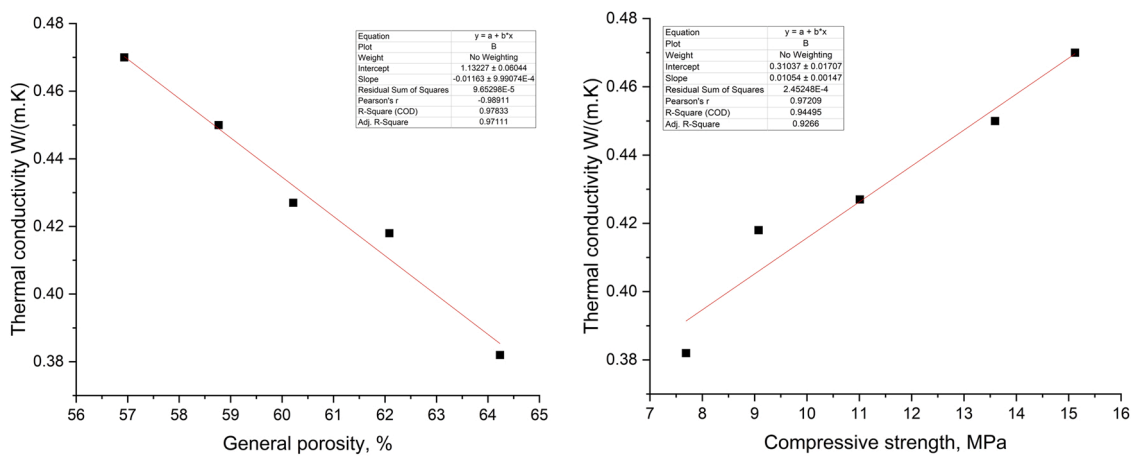


**Fig. 19.** Relationship between general porosity, compressive strength, and thermal conductivity LWSCCC containing aerogel.

aggregates and strength [7]. Agreeing with the previous studies and literature, the combinations of fine EGA were used to achieve higher workability with sufficient strength characteristics. Previously, Yu et al. [28] developed LWSCCC using EGA having a density of 1280–1490 kg/m<sup>3</sup> with 23.3 and 30.2 MPa compressive strength. They measured the mini-slump value about 300 mm with a



4–11 s V-funnel flow time. This study shows that it is possible to prepare LWSCCC even at a lower than  $1000 \text{ kg/m}^3$ , having achieved adequate mechanical strength. Aerogel and expanded glasses are lightweight materials and the use of these materials in cement composite could significantly reduce the density of the cement composite. A higher concentration of aerogel in a composite could lead to a sudden drop in strength due to its poor mechanical performance. Some researchers observed that the use of 80 vol% of aerogel in concrete could lead to a drastic reduction in compression strength to 1 MPa [36,38,59]. Due to the very lightweight density, LWA can float to the top and face segregation problems [6,68]. Li et al. [67] suggested that greater content of fine particle and binding materials could enhance the mortar film thickness leading to improvement in workability. Agreeing with the previous literature, a higher content of binding materials and fine grains of EGA and aerogel were used in the LWSCCC. Due to the use of a high volume of fine particles, there was no visual segregation, and some floating of aerogel particles was observed. However, the addition of aerogel slightly decreased the workability of the composite, but greatly lowered the density and improved the thermal conductivity of the composite. Perhaps entrapped air bubbles by aerogel in the composite mixture enhance the viscosity of LWSCCC, leading to an increase in V-funnel time.

### 3.10. Conclusion

The experimental study investigates the suitability of aerogel particles to produce LWSCCC. From the analysis of the obtained results, the following conclusions can be drawn.

- The increase in fine EGA concentration enhanced the water and superplasticizer demand to maintain the workability of the composite. The W/B ratio and superplasticizer doses play a dominant role in enhancing the workability of LWSCCC, while pozzolanic additions show marginal impacts. The addition of aerogel decreased the slump flow of the composite. It is evident from SEM and porosity results that the inclusion of aerogel in LWSCCC might entrap some air bubbles that might increase the viscosity of the composite, leading to an enhancement in flow time.
- The composite samples containing EGA show a higher risk of water absorption. The inclusion of aerogel increases the total and open porosity of LWSCCC. The total and open porosity of the control sample were calculated 56.93% and 15.72%, respectively which increased to 64.23%, and 19.32% for the A100 sample.
- The porous structured EGA has low strength, and the addition of a greater amount of EGA reduces the strength of the composite. However, the addition of a small amount of natural sand might improve the strength of the composite. As expected, the compressive and flexural strength of aerogel added LWSCCC declined with the enhancement in aerogel concentrations. Almost 49.2% and 34.6% reduction compressive and flexural strength was measured by the addition of aerogel as a replacement of EGA. The lower strength of aerogel weakened adhesion with cement, and increased porosity might lead to a reduction in the strength of aerogel added LWSCCC.
- As expected, the zeolite and fly ash reacted with the cement and slightly impacted the hydration. The presence of ettringite was observed for all LWSCCC samples, but a lower water/binder ratio and the inclusion of zeolite might have accelerated the ettringite formation. XRD and SEM images of the LWSCCC clearly shows the presence of ettringite in the LWSCCC.
- An amorphous aerogel might partially dissolve in the alkaline environment of OPC and perhaps accelerate the growth of hydration products. Through the SEM analysis, aerogel particles and some pores surrounding the aerogel in the composite mixture can be clearly detected. Separation gaps in the ITZ between aerogel and cement paste suggested weaker adhesion of aerogel, while greater adhesion of EGA with cement paste was observed. The separation gaps and pores might enhance the porosity and water absorption of LWSCC.
- The use of expanded glass aggregates combined with aerogel significantly lowers the density of the composite, leading to a decrease in the thermal conductivity of LWSCCC.

### Declaration of Competing Interest

The authors declare that they have no known competing financial interests or personal relationships that could have appeared to influence the work reported in this paper.

### References

- [1] S.K. Adhikary, D.K. Ashish, Ž. Rudžionis, Expanded glass as light-weight aggregate in concrete – a review, *J. Clean. Prod.* 313 (2021), 127848, <https://doi.org/10.1016/j.jclepro.2021.127848>.
- [2] Y. Wu, J.Y. Wang, P.J.M. Monteiro, M.H. Zhang, Development of ultra-lightweight cement composites with low thermal conductivity and high specific strength for energy efficient buildings, *Constr. Build. Mater.* 87 (2015) 100–112, <https://doi.org/10.1016/j.conbuildmat.2015.04.004>.
- [3] T. Cheboub, Y. Senhadji, H. Khelafi, G. Escadeillas, Investigation of the engineering properties of environmentally-friendly self-compacting lightweight mortar containing olive kernel shells as aggregate, *J. Clean. Prod.* 249 (2020), 119406, <https://doi.org/10.1016/j.jclepro.2019.119406>.
- [4] Q.L. Yu, H.J.H. Brouwers, Development of a self-compacting gypsum-based lightweight composite, *Cem. Concr. Compos.* 34 (2012) 1033–1043, <https://doi.org/10.1016/j.cemconcomp.2012.05.004>.
- [5] Y.W. Choi, Y.J. Kim, H.C. Shin, H.Y. Moon, An experimental research on the fluidity and mechanical properties of high-strength lightweight self-compacting concrete, *Cem. Concr. Res.* 36 (2006) 1595–1602, <https://doi.org/10.1016/j.cemconres.2004.11.003>.
- [6] J. Kwasyński, M. Sonebi, S.E. Taylor, Y. Bai, K. Owens, W. Doherty, Influence of the type of coarse lightweight aggregate on properties of semilightweight self-consolidating concrete, *J. Mater. Civ. Eng.* 24 (2012) 1474–1483, [https://doi.org/10.1061/\(asce\)mt.1943-5533.0000527](https://doi.org/10.1061/(asce)mt.1943-5533.0000527).
- [7] S.K. Adhikary, Z. Rudžionis, Influence of expanded glass aggregate size, aerogel and binding materials volume on the properties of lightweight concrete, *Mater. Today Proc.* 32 (2020) 712–718, <https://doi.org/10.1016/j.matpr.2020.03.323>.

- [8] Q.L. Yu, P. Spiesz, H.J.H. Brouwers, Development of cement-based lightweight composites - part 1: mix design methodology and hardened properties, *Cem. Concr. Compos.* 44 (2013) 17–29, <https://doi.org/10.1016/j.cemconcomp.2013.03.030>.
- [9] N. Abbas, H.R. Khalid, G. Ban, H.T. Kim, H.K. Lee, Silica aerogel derived from rice husk: an aggregate replacer for lightweight and thermally insulating cement-based composites, *Constr. Build. Mater.* 195 (2019) 312–322, <https://doi.org/10.1016/j.conbuildmat.2018.10.227>.
- [10] G. Jia, Z. Li, Influence of the aerogel/expanded perlite composite as thermal insulation aggregate on the cement-based materials: Preparation, property, and microstructure, *Constr. Build. Mater.* 273 (2021), 121728, <https://doi.org/10.1016/j.conbuildmat.2020.121728>.
- [11] K.L. Huang, S.J. Li, P.H. Zhu, Effect of early curing temperature on the tunnel fire resistance of self-compacting concrete coated with aerogel cement paste, *Materials* 14 (2021) 5782, <https://doi.org/10.3390/ma14195782>.
- [12] T. Gao, B.P. Jelle, A. Gustavsen, S. Jacobsen, Aerogel-incorporated concrete: an experimental study, *Constr. Build. Mater.* 52 (2014) 130–136, <https://doi.org/10.1016/j.conbuildmat.2013.10.100>.
- [13] S.K. Adhikary, D.K. Ashish, Z. Rudzionis, Aerogel based thermal insulating cementitious composites: a review, *Energy Build.* 245 (2021), 111058, <https://doi.org/10.1016/j.enbuild.2021.111058>.
- [14] S.K. Adhikary, Z. Rudzionis, S. Tučkutė, D.K. Ashish, Effects of carbon nanotubes on expanded glass and silica aerogel based lightweight concrete, *Sci. Rep.* 11 (2021) 2104, <https://doi.org/10.1038/s41598-021-81665-y>.
- [15] X. Wang, P. Zhu, S. Yu, H. Liu, Y. Dong, X. Xu, Effect of moisture content on tunnel fire resistance of self-compacting concrete coated with aerogel mortar, *Mag. Concr. Res.* 73 (2021) 1071–1080, <https://doi.org/10.1680/jmacr.19.00436>.
- [16] P. Zhu, Z. Jia, X. Wang, C. Chen, H. Liu, X. Xu, Density dependence of tunnel fire resistance for aerogel-cement mortar coatings, *J. Wuhan. Univ. Technol. Mater. Sci. Ed.* 35 (2020) 598–604, <https://doi.org/10.1007/s11595-020-2296-3>.
- [17] P. Zhu, X. Xu, H. Liu, S. Liu, C. Chen, Z. Jia, Tunnel fire resistance of self-compacting concrete coated with SiO<sub>2</sub> aerogel cement paste under 2.5h HC fire loading, *Constr. Build. Mater.* 239 (2020), 117857, <https://doi.org/10.1016/j.conbuildmat.2019.117857>.
- [18] Specification and Guidelines for Self-Compacting Concrete, EFNARC, Rep. from EFNARC, (2002) 32.
- [19] M.L. Torres, P.A. García-Ruiz, Lightweight pozzolanic materials used in mortars: evaluation of their influence on density, mechanical strength and water absorption, *Cem. Concr. Compos.* 31 (2009) 114–119, <https://doi.org/10.1016/j.cemconcomp.2008.11.003>.
- [20] Q.L. Yu, P. Spiesz, H.J.H. Brouwers, Ultra-lightweight concrete: conceptual design and performance evaluation, *Cem. Concr. Compos.* 61 (2015) 18–28, <https://doi.org/10.1016/j.cemconcomp.2015.04.012>.
- [21] G. Bumanis, D. Bajare, J. Locs, A. Korjakins, Alkali-silica reactivity of expanded glass granules in structure of lightweight concrete, *IOP Conf. Ser. Mater. Sci. Eng.* 47 (2013) 12022, <https://doi.org/10.1088/1757-899x/47/1/012022>.
- [22] R.W. Floyd, W.M. Hale, J.C. Bymaster, Effect of aggregate and cementitious material on properties of lightweight self-consolidating concrete for prestressed members, *Constr. Build. Mater.* 85 (2015) 91–99, <https://doi.org/10.1016/j.conbuildmat.2015.03.084>.
- [23] T.Z.H. Ting, M.E. Rahman, H.H. Lau, Sustainable lightweight self-compacting concrete using oil palm shell and fly ash, *Constr. Build. Mater.* 264 (2020), 120590, <https://doi.org/10.1016/j.conbuildmat.2020.120590>.
- [24] S.K. Adhikary, Z. Rudzionis, D. Vaičiukynienė, Development of flowable ultra-lightweight concrete using expanded glass aggregate, silica aerogel, and prefabricated plastic bubbles, *J. Build. Eng.* 31 (2020), 101399, <https://doi.org/10.1016/j.jobbe.2020.101399>.
- [25] S.N. Shah, K.H. Mo, S.P. Yap, M.K.H. Radwan, Effect of micro-sized silica aerogel on the properties of lightweight cement composite, *Constr. Build. Mater.* 290 (2021), 123229, <https://doi.org/10.1016/j.conbuildmat.2021.123229>.
- [26] S. Kim, J. Seo, J. Cha, S. Kim, Chemical retreating for gel-typed aerogel and insulation performance of cement containing aerogel, *Constr. Build. Mater.* 40 (2013) 501–505, <https://doi.org/10.1016/j.conbuildmat.2012.11.046>.
- [27] A. Venkateswara Rao, M.M. Kulkarni, D.P. Amalnerkar, T. Seth, Surface chemical modification of silica aerogels using various alkyl-alkoxy/chloro silanes, *Appl. Surf. Sci.* 206 (2003), [https://doi.org/10.1016/S0169-4332\(02\)01232-1](https://doi.org/10.1016/S0169-4332(02)01232-1).
- [28] J. Zach, M. Sedlmajer, J. Hroudova, A. Nevařil, Technology of concrete with low generation of hydration heat, *Procedia Eng.* 65 (2013) 296–301, <https://doi.org/10.1016/j.proeng.2013.09.046>.
- [29] K. Gorospe, E. Booya, H. Ghaednia, S. Das, Effect of various glass aggregates on the shrinkage and expansion of cement mortar, *Constr. Build. Mater.* 210 (2019) 301–311, <https://doi.org/10.1016/j.conbuildmat.2019.03.192>.
- [30] J. Lu, J. Jiang, Z. Lu, J. Li, Y. Niu, Y. Yang, Pore structure and hardened properties of aerogel/cement composites based on nanosilica and surface modification, *Constr. Build. Mater.* 245 (2020), 118434, <https://doi.org/10.1016/j.conbuildmat.2020.118434>.
- [31] C. Lian, Y. Zhuge, S. Beecham, The relationship between porosity and strength for porous concrete, *Constr. Build. Mater.* 25 (2011) 4294–4298, <https://doi.org/10.1016/j.conbuildmat.2011.05.005>.
- [32] P. Spiesz, Q.L. Yu, H.J.H. Brouwers, Development of cement-based lightweight composites - part 2: durability-related properties, *Cem. Concr. Compos.* 44 (2013) 30–40, <https://doi.org/10.1016/j.cemconcomp.2013.03.029>.
- [33] M. Kurpińska, T. Ferenc, Effect of porosity on physical properties of lightweight cement composite with foamed glass aggregate, *ITM Web Conf.* 15 (2017) 06005.
- [34] A. Yousefi, W. Tang, M. Khavarian, C. Fang, S. Wang, Thermal and mechanical properties of cement mortar composite containing recycled expanded glass aggregate and nano titanium dioxide, *Appl. Sci.* 10 (2020) 2246, <https://doi.org/10.3390/app10072246>.
- [35] D. Rumsys, E. Spudulis, D. Bacinskas, G. Kaklauskas, Compressive strength and durability properties of structural lightweight concrete with fine expanded glass and/or clay aggregates, *Materials* 11 (2018), <https://doi.org/10.3390/ma11122434>.
- [36] P. Zhu, S. Yu, C. Cheng, S. Zhao, H. Xu, Durability of silica aerogel cementitious composites - Freeze-thaw resistance, water resistance and drying shrinkage, *Adv. Cem. Res.* 32 (2020) 527–536, <https://doi.org/10.1680/jadcr.18.00145>.
- [37] Z. hui Liu, F. Wang, Z. ping Deng, Thermal insulation material based on SiO<sub>2</sub> aerogel, *Constr. Build. Mater.* 122 (2016) 548–555, <https://doi.org/10.1016/j.conbuildmat.2016.06.096>.
- [38] S. Ng, B.P. Jelle, L.L.C. Sandberg, T. Gao, Ó.H. Wallelevik, Experimental investigations of aerogel-incorporated ultra-high performance concrete, *Constr. Build. Mater.* 77 (2015) 307–316, <https://doi.org/10.1016/j.conbuildmat.2014.12.064>.
- [39] F. Chen, Y. Zhang, J. Liu, X. Wang, P.K. Chu, B. Chu, N. Zhang, Fly ash based lightweight wall materials incorporating expanded perlite/SiO<sub>2</sub> aerogel composite: towards low thermal conductivity, *Constr. Build. Mater.* 249 (2020), 118728, <https://doi.org/10.1016/j.conbuildmat.2020.118728>.
- [40] A. Hanif, P. Parthasarathy, Z. Li, (2017-Utilizing Fly Ash Cenosphere and Aerogel for. pdf), 11 (2017) 84–90.
- [41] S.Y. Chung, P. Sikora, D.J. Kim, M.E. El Madawy, M. Abd Elrahman, Effect of different expanded aggregates on durability-related characteristics of lightweight aggregate concrete, *Mater. Charact.* 173 (2021), 110907, <https://doi.org/10.1016/j.matchar.2021.110907>.
- [42] S.Y. Chung, M. Abd Elrahman, J.S. Kim, T.S. Han, D. Stephan, P. Sikora, Comparison of lightweight aggregate and foamed concrete with the same density level using image-based characterizations, *Constr. Build. Mater.* 211 (2019) 988–999, <https://doi.org/10.1016/j.conbuildmat.2019.03.270>.
- [43] M. Limbachiya, M.S. Meddah, S. Fotiadou, Performance of granulated foam glass concrete, *Constr. Build. Mater.* 28 (2012) 759–768, <https://doi.org/10.1016/j.conbuildmat.2011.10.052>.
- [44] M. Kurpińska, L. Kulak, Predicting performance of lightweight concrete with granulated expanded glass and ash aggregate by means of using artificial neural networks, *Materials* 12 (2019), <https://doi.org/10.3390/ma12122002>.
- [45] T. Hemalatha, A. Ramaswamy, A review on fly ash characteristics – towards promoting high volume utilization in developing sustainable concrete, *J. Clean. Prod.* 147 (2017) 546–559, <https://doi.org/10.1016/j.jclepro.2017.01.114>.
- [46] B. Ahmadi, M. Shekarchi, Use of natural zeolite as a supplementary cementitious material, *Cem. Concr. Compos.* 32 (2010) 134–141, <https://doi.org/10.1016/j.cemconcomp.2009.10.006>.
- [47] S.Y.N. Chan, X. Ji, Comparative study of the initial surface absorption and chloride diffusion of high performance zeolite, silica fume and PFA concretes, *Cem. Concr. Compos.* 21 (1999) 293–300, [https://doi.org/10.1016/S0958-9465\(99\)00010-4](https://doi.org/10.1016/S0958-9465(99)00010-4).

- [48] K. Guo, H. Song, X. Chen, X. Du, L. Zhong, Graphene oxide as an anti-shrinkage additive for resorcinol-formaldehyde composite aerogels, *Phys. Chem. Chem. Phys.* 16 (2014) 11603–11608, <https://doi.org/10.1039/c4cp00592a>.
- [49] L. Wang, P. Liu, Q. Jing, Y. Liu, W. Wang, Y. Zhang, Z. Li, Strength properties and thermal conductivity of concrete with the addition of expanded perlite filled with aerogel, *Constr. Build. Mater.* 188 (2018) 747–757, <https://doi.org/10.1016/j.conbuildmat.2018.08.054>.
- [50] H. Li, P. Zang, H. Liu, K. Cao, X. Liao, D. Wei, B. Zhang, H. Li, J. Wang, Preparation and heat insulation of Geminihalloysite aerogel/concrete composites, *J. Polym. Eng. 41* (2021) 387–396, <https://doi.org/10.1515/polyeng-2020-0317>.
- [51] S.K. Adhikary, Z. Rudzionis, S. Tučkutė, D.K. Ashish, Effects of carbon nanotubes on expanded glass and silica aerogel based lightweight concrete, *Sci. Rep.* 11 (2021) 2104, <https://doi.org/10.1038/s41598-021-81665-y>.
- [52] P.-H. Zhu, Y.-Q. Sun, Experimental study on the influence of particle size of the SiO<sub>2</sub> aerogel on properties of silica aerogel tunnel fireproof mortar, *DEStech Trans. Mater. Sci. Eng.* (2017) 2–7, <https://doi.org/10.12783/dtmse/icmsea/mce2017/10858>.
- [53] A. Soares, M. Julio, I. Flores-Colen, L. Ilharco, J. De Brito, J. Gaspar Martinho, Water-resistance of mortars with lightweight aggregates, *Key Eng. Mater.* 634 (2015) 46–53, <https://doi.org/10.4028/www.scientific.net/KEM.634.46>.
- [54] B.H. Spratt, *Lightweight Aggregate Concrete*, Civ. Eng., London, 1984, [https://doi.org/10.1016/0016-0032\(45\)90197-9](https://doi.org/10.1016/0016-0032(45)90197-9).
- [55] G. Bumanis, D. Bajare, J. Locs, A. Korjakins, Alkali-silica reactivity of foam glass granules in structure of lightweight concrete, *Constr. Build. Mater.* 47 (2013) 274–281, <https://doi.org/10.1016/j.conbuildmat.2013.05.049>.
- [56] P. Zhu, S. Brunner, S. Zhao, M. Griffa, A. Leemann, N. Toropovs, A. Malekos, M.M. Koebel, P. Lura, Study of physical properties and microstructure of aerogel-cement mortars for improving the fire safety of high-performance concrete linings in tunnels, *Cem. Concr. Compos.* 104 (2019), 103414, <https://doi.org/10.1016/j.cemconcomp.2019.103414>.
- [57] C. Hai-li, Influence on the Performances of Foamed Concrete by Silica Aerogels, *Am. J. Civ. Eng.* 3 (2015) 183, <https://doi.org/10.11648/j.ajce.20150305.18>.
- [58] M. de Fátima Júlio, L.M. Ilharco, A. Soares, I. Flores-Colen, J. de Brito, Silica-based aerogels as aggregates for cement-based thermal renders, *Cem. Concr. Compos.* 72 (2016) 309–318, <https://doi.org/10.1016/j.cemconcomp.2016.06.013>.
- [59] S. Ng, B.P. Jelle, T. Stæhli, Calcined clays as binder for thermal insulating and structural aerogel incorporated mortar, *Cem. Concr. Compos.* 72 (2016) 213–221, <https://doi.org/10.1016/j.cemconcomp.2016.06.007>.
- [60] J. ping Zuo, Z. jie Hong, Z. qiang Xiong, C. Wang, H. qiang Song, Influence of different W/C on the performances and hydration progress of dual liquid high water backfilling material, *Constr. Build. Mater.* 190 (2018) 910–917, <https://doi.org/10.1016/j.conbuildmat.2018.09.146>.
- [61] M.D.M. Alonso, M. Palacios, F. Puertas, Effect of polycarboxylate-ether admixtures on calcium aluminate cement pastes. Part I: compatibility studies, *Ind. Eng. Chem. Res.* 52 (2013) 17323–17329, <https://doi.org/10.1021/ie401615t>.
- [62] R. Snellings, G. Mertens, Ö. Cizer, J. Elsen, Early age hydration and pozzolanic reaction in natural zeolite blended cements: Reaction kinetics and products by in situ synchrotron X-ray powder diffraction, *Cem. Concr. Res.* 40 (2010) 1704–1713, <https://doi.org/10.1016/j.cemconres.2010.08.012>.
- [63] A. Lamy-Mendes, A.D.R. Pontinha, P. Alves, P. Santos, L. Durães, Progress in silica aerogel-containing materials for buildings' thermal insulation, *Constr. Build. Mater.* 286 (2021), 122815, <https://doi.org/10.1016/j.conbuildmat.2021.122815>.
- [64] S.N. Shah, K.H. Mo, S.P. Yap, M.K.H. Radwan, Towards an energy efficient cement composite incorporating silica aerogel: a state of the art review, *J. Build. Eng.* 44 (2021), 103227, <https://doi.org/10.1016/j.jobe.2021.103227>.
- [65] A. Hanif, S. Diao, Z. Lu, T. Fan, Z. Li, Green lightweight cementitious composite incorporating aerogels and fly ash cenospheres - mechanical and thermal insulating properties, *Constr. Build. Mater.* 116 (2016) 422–430, <https://doi.org/10.1016/j.conbuildmat.2016.04.134>.
- [66] P.F. Bergmann Becker, C. Effting, A. Schackow, Lightweight thermal insulating coating mortars with aerogel, EPS, and vermiculite for energy conservation in buildings, *Cem. Concr. Compos.* 125 (2022), 104283, <https://doi.org/10.1016/j.cemconcomp.2021.104283>.
- [67] J. Li, Y. Chen, C. Wan, A mix-design method for lightweight aggregate self-compacting concrete based on packing and mortar film thickness theories, *Constr. Build. Mater.* 157 (2017) 621–634, <https://doi.org/10.1016/j.conbuildmat.2017.09.141>.
- [68] S.K. Adhikary, Z. Rudzionis, Influence of expanded glass aggregate size, aerogel and binding materials volume on the properties of lightweight concrete, *Mater. Today Proc.* 32 (2020) 712–718, <https://doi.org/10.1016/j.matpr.2020.03.323>.